The Journal of Engineering

Research Article

IET Journals
The Institution of Engineering and Technology

Online impedance spectroscopy estimation of a dc–dc converter connected battery using a switched capacitor-based balancing circuit

eISSN 2051-3305
Received on 11th June 2019
Accepted on 24th June 2019
doi: 10.1049/joe.2018.8069
www.ietdl.org

Mina Abedi Varnosfaderani[1] ✉, *Dani Strickland*[1]

[1]*Loughborough University, Crest Department, Epinal Way, Loughborough LE11 3TU, UK*

✉ *E-mail: m.abedi-varnosfaderani@lboro.ac.uk*

Abstract: This study investigates a novel method of undertaking online electrochemical impedance spectroscopy measurements to estimate battery impedance across the frequency range using a battery balancing circuit. A switched capacitor balancing system is used to generate an excitation signal of low-frequency of variable values from which battery voltage and current can be measured to estimate the impedance.

1 Introduction

Electrochemical impedance spectroscopy (EIS) is a method of determining impedance across a frequency spectrum to try and understand electrochemical behaviour in a test piece such as a battery. It is typical to undertake EIS offline – but online techniques offer a more useful long-term focus for understanding degradation in real time. The high accuracy of the offline EIS technique allows it to be used as a benchmark to validate other techniques.

Recent work in this area [1] has attempted to classify the different areas of on-line EIS measurement that have been undertaken as shown in Fig. 1. Some attempts to replicate an EIS method on-line have been undertaken [1–8]. The authors of [1, 9–12] use a separate excitation circuit for online EIS excitation. This technique requires additional hardware and there are extra costs involved with the implementation. The authors of [1–4, 6, 8, 13–16] use the power electronics circuitry to generate the EIS excitation signal. The method of introducing a small excitation signal through the dc/dc power electronics is primarily a function of different forms of control. These methods can be split into those that occur under diagnostic mode [14] and those under normal operational mode. The normal operational mode can also be split into different methods used to introduce a low-frequency signal. These methods include using a variable voltage set point [7] and a variable duty cycle [3, 6, 8, 13–15]. Some initial work has been undertaken to look at using the battery balancing circuit to generate the excitation signal. Koch *et al*. [15] used a balancing resistor with a switch to excite the battery. This method is sensitive to the balancing current and can only discharge the battery. The authors of [4, 16] use an inductive-based battery balancing system for online EIS measurement. However, the balancing circuit is tied up with the power electronic circuit and therefore it is less straightforward to connect the battery directly to a dc/dc converter or dc/ac converter. This work is novel as it looks in detail at the use of a capacitive-based battery balancing method for looking at on-line EIS measurements.

In this study, a standard switched capacitor balancing system is designed and sized to generate the low-frequency excitation signal needed for EIS measurement and analysis. The switched capacitor system is connected to the battery to balance across several cells. The impedance of the battery is calculated by harmonic analysis of the measured battery current and voltage data at the excitation frequency point. The frequency range is swept to generate an EIS impedance measurement over the frequency range. The technique is conducted on-line with the battery system operating under normal operation. The schematic figure of two battery cells and converter with the switched capacitor balancing technique is shown in Fig. 2.

The remainder of this paper is organised as follows: Section 2 looks at the theoretical analysis of this technique, Section 3 presents the modelling of the technique. Section 4 presents experimentally derived results and looks at validating the waveforms and the impedance calculated by comparing this to that calculated by offline EIS measurement.

2 Theory

The main research question to be addressed is to determine how best to inject a low-frequency waveform into the battery without the use of additional excitation hardware, for the EIS calculation, while at the same time ensuring the normal operation of the power system. In this study, two battery cells are connected to a typical dc/dc converter and a battery balancing system. This is done to assist with low scale, low-cost proof of concept. The two series battery cells are connected to the load through a boost converter while the terminals of each battery are connected to a balancing circuit (see Fig. 2). In this battery balancing circuit, one capacitor and four metal oxide semiconductor field effect transistor (MOSFET) switches are used. The capacitor and switches M1–M4 were operated to balance the batteries while at the same time producing a low-frequency excitation signal.

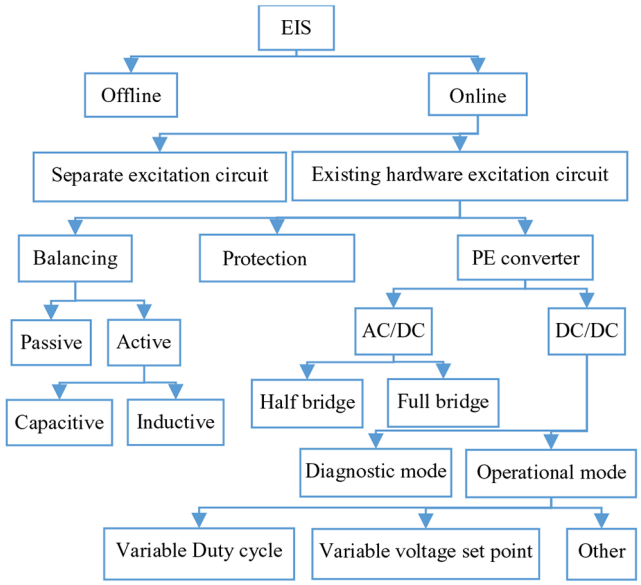

Fig. 1 *Different battery EIS methods*

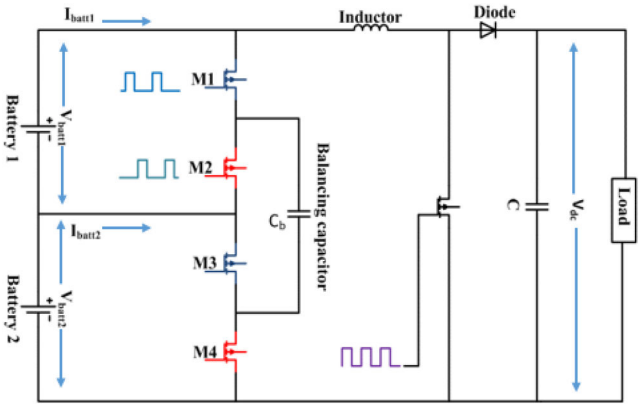

Fig. 2 *Switched capacitor battery balancing circuit*

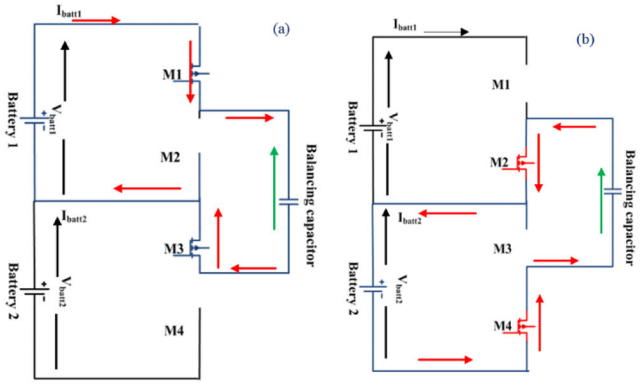

Fig. 3 *Switching capacitor battery balancing circuit operation*
(a) Stage 1 – charging, ***(b)*** Stage 2 – discharging

The value of the capacitor was chosen so that the low-frequency switching allows energy transfer between the two batteries. The time constant of the battery balancing system is set to ∼0.3 ms so over several high-frequency switching operations the capacitor will have charged. This was done by assuming a circuit resistance of ∼30 mΩ made up of battery resistance, capacitor equivalent series resistance (ESR), MOSFETs on resistance, leads and connectors and choosing a capacitor at 10 mF. The system works in two stages as shown in Fig. 3.

When the voltage of battery 1 is higher than battery 2.

(i) Switches M1 and M3 are turned on and switches M2 and M4 are turned off, the capacitor will be connected in parallel with battery 1 through switches M1 and M3 (see Fig. 3*a*). The capacitor then starts to charge from battery 1.

(ii) Switches M2 and M4 are turned on and switches M1 and M3 are turned off, the capacitor will be connected in parallel with battery 2 through switches M2 and M4 (see Fig. 3*b*). The capacitor starts to discharge to battery 2.

Two pulse signals with the duty cycle of <0.5 are used for controlling the switches M1–M4 [17]. The reason for choosing a duty cycle <0.5 is to avoid a short-circuit condition or current shoot-through when all switches are turned on at once. In this system, a duty cycle of 0.45 was used for the pulse signals. One pulse signal is used for charging the capacitor from the battery cell with a higher voltage. The other pulse signal is used for discharging the capacitor to the battery cell with a lower voltage. The frequency of the battery balancing is at a lower frequency than the boost converter switching frequency, to induce the low-frequency excitation signal.

In this study, the boost converter is operating open loop with a fixed duty cycle, *d*. However, the battery voltages are subject to a small perturbation caused by the balancing capacitor charging and discharging low-frequency injection as shown in Fig. 4. The final waveform seen by the battery is a superposition signal of the converter saw tooth pattern and the battery balancing signal as

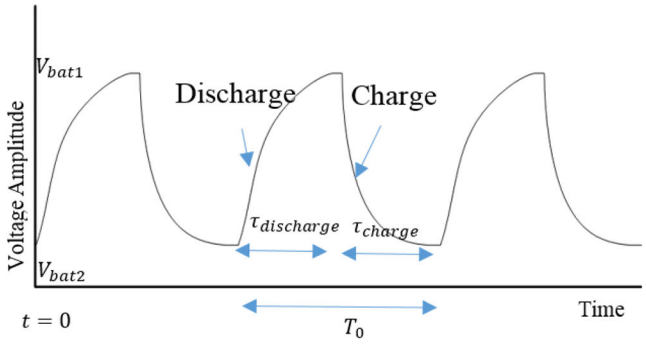

Fig. 4 *Charging and discharging voltage waveform for the balancing capacitor at the low frequency*

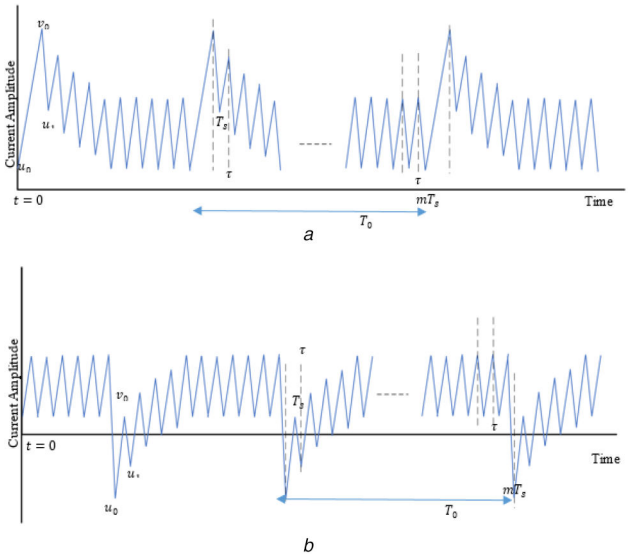

Fig. 5 *Current waveform for a battery balancing method*
(a) Battery 1 discharge current, ***(b)*** Battery 2 charge current

shown in Fig. 5. The minimum voltage of the balancing capacitor is equal to the battery with lower voltage value (V_{bat2}), and the maximum value of the balancing capacitor is equal to the battery with higher-voltage value (V_{bat1}).

When the switches M1 and M3 are on the capacitor charges from battery 1 with a current, i_{cb_charge} equal to

$$i_{cb\_charge} = C\frac{(V_{bat1} - V_{bat2})}{\tau_c}e^{-t/\tau_c} \quad (1)$$

When the switches M2 and M4 are on the capacitor discharges to battery 2, with a current, $i_{cb\_discharge}$ equal to

$$i_{cb\_discharge} = -C\frac{(V_{bat1} - V_{bat2})}{\tau_c}e^{-t/\tau_c} \quad (2)$$

where V_{bat1} is the voltage of the battery with the higher voltage and V_{bat2} is the voltage of the lower value voltage battery, C is the battery balancing capacitor and τ_c is the time constant of the circuit based on C and the resistance of the charging/discharging loop.

As the battery current and voltage are a function of the boost converter current and the current caused by the battery balancing circuit, the low-frequency component of the measured current needs to be extracted using Fourier transforms. The current on the battery with the higher voltage increases at each low-frequency interval f_0 as the capacitor current is added to the boost converter current. While the current on the battery with the lower voltage decreases with each low-frequency switched period when connected to the capacitor as the capacitor is used to offset the boost converter current and charge the battery. Fig. 5 illustrates the charge and discharge current of battery 1 and battery 2. The current

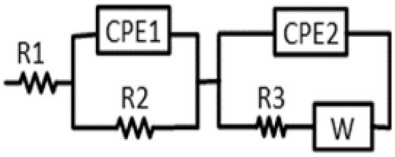

Fig. 6 *Battery equivalent circuit*

Table 1 Battery parameters estimated from offline EIS and converter details

Battery parameters	Values	Boost converter components	Specifications
R_1, Ω	0.0069	inductance	380 μH, 20 A, toroidal
R_2, Ω	0.0056	capacitance	13,600 μF, 16 V electrolytic
R_3, Ω	0.00089	load	16 Ω resistor
CPE_1	3.36	switch MOSFET	FDPF045N10A, 100 V, 67 A, 4.5 mΩ
CPE_2	0.43	diode	HER204G rectifier diode (max 2A)

and voltage of each battery need to be analysed separately to calculate the impedance of each individual cell.

There is a negligible extra boost inductor current as the current from the capacitor will act to charge/discharge the batteries. This capacitor current is dependent on the difference in battery voltage between the cells, so it is not fixed with time but varies as a function of the voltage difference. This gives rise to two points:

- The low-frequency excitation is significantly reduced if the battery voltages in the cells are close. This is likely to be okay as monitoring is most valuable when a battery is degraded and therefore likely to discharge faster causing the voltage to drop quicker than that from normal cells.
- The low-frequency excitation can be adjusted based on voltage difference to help with equalisation and controlling the ripple on the battery. This is because the current in (1) and (2) is dependent on the time period that the capacitor is switched in and out (which in turn is dependent on the excitation frequency) to keep a constant ripple current.
- The method is dependent on a dV/dt change in the capacitor. It is not clear if this technique can be used with a resistive balancing method similar to [15].

The extra ripple current in each battery can be calculated by considering the increase in current due to the balancing capacitor current from the equations above. The ripple increases as a function of the impedance of the battery. As the battery degrades, its impedance increases (resulting in a reduced τ) leading to a less accurate calculation.

The converter current over one switching cycle in boost mode in an ideal converter for battery 1 can be calculated traditionally as

$$\Delta i_{\text{on}} = \frac{1}{L}(V_{\text{bat1}} + V_{\text{bat2}})\text{d}T_{\text{s}} \tag{3}$$

$$\Delta i_{\text{off}} = \frac{1}{L}(V_{\text{bat1}} + V_{\text{bat2}} - V_{\text{dc}})(T_{\text{s}} - dT_{\text{s}}) \tag{4}$$

3 Modelling

In order to help understand the operation of the circuit with respect to the theory and experimental work, it is helpful to look at modelling the circuit within a suitable package. To undertake a circuit simulation, the impedance of two A123 lithium-ion phosphate batteries with 2.5 Ah capacity and 3.2 V nominal voltage, for use in the model was found by EIS measurement and represented in a MATLAB simulation as an equivalent circuit typified by that in [18]. Fig. 6 shows the battery equivalent circuit model. The battery component values of both batteries were considered the same and were estimated from the off-line EIS measurement of the battery at 100% state of charge at room temperature.

The switched capacitor balancing method was modelled for the balancing of two battery cells. To balance these two cells, four

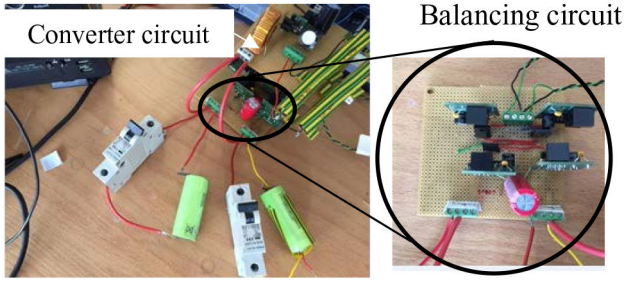

Fig. 7 *Experimental set-up*

MOSFET switching components with a 10 mF capacitor were used. The value of this balancing capacitor affects the speed of the balancing time. Some authors [17, 19] also use a series inductance for soft-switching of the battery balancing. They chose the capacitor values based on the resonance circuit design. In this work, a series inductance was not used and is considered further work. The boost converter was designed such that it operated in continuous conduction mode at a switching frequency of 2 kHz with a duty cycle of 0.6 for a battery voltage of 3.21 V. The estimated battery equivalent circuit parameters and boost converter components used in the modelling are shown in Table 1.

4 Experimental result

Fig. 7 shows the experimental setup used to look at on-line low-frequency impedance measurement as described above. The impedance at different frequencies was calculated by measuring the battery voltage and current using a Lecroy 100 MHz current probe and a Tektronix P2220 200 MHz voltage probe for convenience, but an ACS712 current sensor and an IL300 voltage sensor measurement device linked to the controller have also been used to get the same results.

The experimentally captured battery current and voltage waveforms both without the battery balancing and with the balancing for a low-frequency point of 125 Hz are shown in Fig. 8. The resulting ripple current in batteries 1 and 2 is a result of the superposition of the balancing capacitor charging and discharging currents with the converter saw tooth waveform. The current ripple of both batteries follows an exponential decay related to the time constant of the capacitor balancing circuit.

The circuit was run with a boost converter switching frequency of 2 kHz, a duty cycle of 0.6 in continuous mode. The battery balancing circuit operates with a duty cycle of 45% for switches M1 and M3 and 45% for switches M2 and M4. Table 2 represents the comparison of the key parameters of the experimental results at the low frequency of 125 Hz against the MATLAB model simulation results under the same conditions.

The results show that the experimental model of the converter and balancing circuit are performing in a manner similar to the simulation. Within the modelling, the non -ideal and non-linear components present in the experimental setup including the diode,

MOSFET, and ESR resistances are not included which explains the differences in current.

The average value of the load voltage, current and the boost ratio of the circuit remain the same as the base circuit under both conditions in Fig. 8. In order to capture these waveforms, the batteries were set to have a large difference in voltage. This is because the resistance in the experimental circuit is greater than that in simulation which is based on an ideal case and as such (2) indicates that charging current will be reduced. In this example, the voltage value of 43.6 mV for battery 2 is not practical and is used at this time only to show proof of concept. Further work is required to determine a better way to calculate the impedance of both batteries with a lower voltage difference.

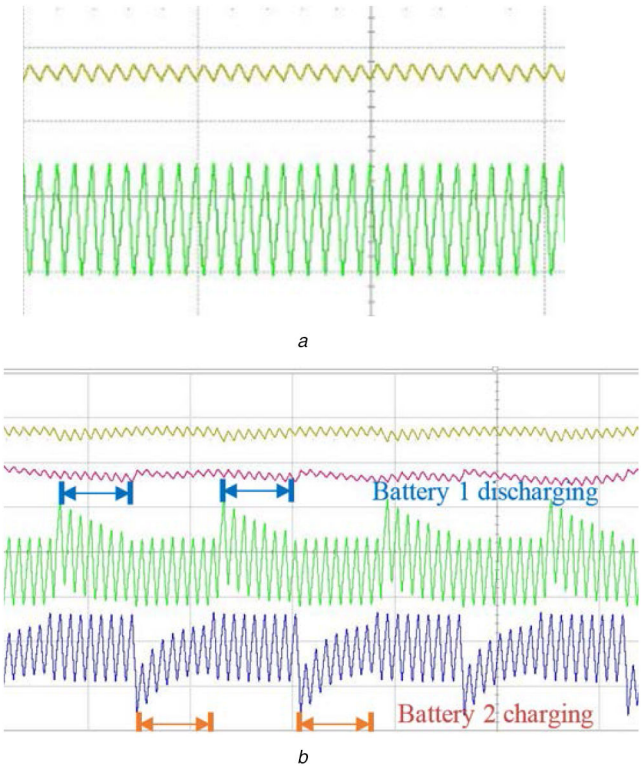

Fig. 8 *Li-ion battery waveforms – battery 1 voltage (yellow) and battery 2 voltage (red) waveforms (top), battery 1 current (green) and battery 2 current (blue) waveforms (bottom), when the system is operating with*
(a) No battery balancing, ***(b)*** Battery balancing operating at 125 Hz

Fig. 9 shows the battery current harmonic analysis showing the boost converter switching frequency of 2 kHz and battery balancing circuit low-frequency of 125 Hz. Both the low frequency of 125 Hz and the switching frequency of 2 kHz harmonics are extracted from the experimentally measured current waveform.

The extracted low-frequency current and voltage harmonics measured while the battery is operational are used to calculate the complex impedance to produce a Nyquist plot. This is compared to an off-line EIS measurement. Fig. 10 shows the calculated complex impedance, amplitude and phase plots of the higher voltage li-ion battery. Data from experimental tests and simulation have similar values to that from offline EIS data.

5 Conclusions

This study presented an analysis and implementation of a method of inducing a low-frequency excitation signal in hardware using battery balancing hardware. The measurements were used to look at different circuit operations, the ripple current increase and its dependency on other variables. The methodology has been experimentally validated by comparing a Nyquist plot of a battery produced using this methodology to that produced using offline EIS measurement. The results are a promising indicating that it may be possible to generate a low-frequency excitation signal in order to undertake on-line EIS measurement using the battery balancing circuitry. However, there are potential disadvantages to this method. The battery balancing used in this work needed a clear voltage difference between two battery cells to detect a signal and the results from the battery with the lower voltage were not as good. There is scope for future work to look at other alternative battery balancing methods from the published literature to produce a low-frequency excitation signal for impedance measurement. However, this study provides a starting point for further investigation in this area.

Table 2 Comparison of base circuit data with the battery balancing circuit at 125 Hz

	Experimental			
	Fixed duty cycle		Battery balancing circuit connected to the converter	
	Average value	Peak–peak ripple	Average value	Peak–peak ripple
I_L	1.18 A	1.49 A	1.18 A	1.59 A
I_{bat1}	1.18 A	1.49 A	1.25 A	2.44 A
I_{bat2}			0.99 A	2.35 A
V_{bat1}	3.21 V	12.45 mV	3.18 V	17.7 mV
V_{bat2}			43.6 mV	26.7 mV
I_{load}	420 mA	10 mA	397 mA	7 mA
V_{dc}	6.89 V	67 mV	6.8 V	86 mV

	Simulation			
	Fixed duty cycle		Battery balancing circuit connected to the converter	
	Average value	Peak–peak ripple	Average value	Peak–peak ripple
I_L	1.55 A	2.42 A	1.56 A	2.73 A
I_{bat1}	1.55 A	2.42 A	1.8 A	3.51 A
I_{bat2}			1.4 A	3.88 A
V_{bat1}	3.21 V	16.8 mV	1.7 V	25 mV
V_{bat2}			1.51 V	26.7 mV
I_{load}	456 mA	0.7 mA	455 mA	0.8 mA
V_{dc}	7.3 V	11.1 mV	7.3 V	12.5 mV

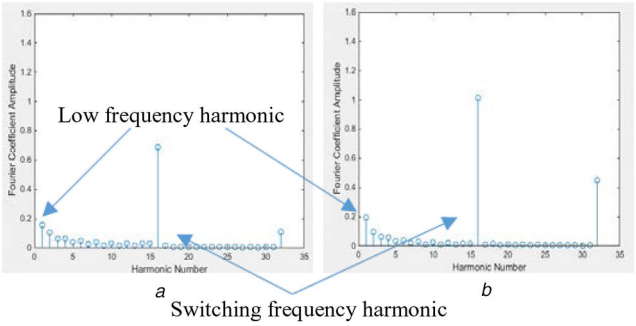

Fig. 9 *Harmonics of the Li-ion battery1 current signal with a balancing capacitor at a low frequency of 125 Hz*
(a) Experimentally derived, ***(b)*** Theoretically derived

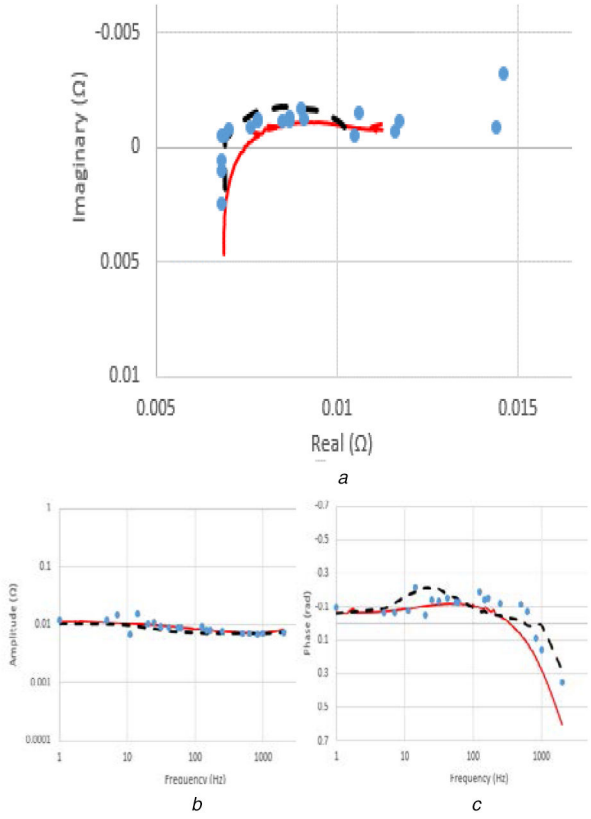

Fig. 10 *Impedance plots of the Li-ion battery with EIS (red), simulation (black), and experimental validation (blue dots)*
(a) Impedance Nyquist plot, ***(b)*** Impedance amplitude bode plot, ***(c)*** Impedance phase bode plot

6 Acknowledgments

This paper was presented at the 9th International Conference on Power Electronics, Machines and Drives (PEMD 2018). The authors would like to thank the EPSRC (project MANIFEST) for their contribution to this work.

7 References

[1] Koch, R., Kuhn, R., Zilberman, I., *et al.*: 'Electrochemical impedance spectroscopy for online battery monitoring – power electronics control'. 2014 16th European Conf. on Power Electronics and Applications (EPE'14-ECCE Europe), Lappeenranta, Finland, 2014, pp. 1–10

[2] Howey, D.A., Mitcheson, P.D., Yufit, V., *et al.*: 'Online measurement of battery impedance using motor controller excitation', *IEEE Trans. Veh. Technol.*, 2014, **63**, (6), pp. 2557–2566

[3] Wangxin, H., Qahouq, J.A.: 'An online battery impedance measurement method using DC–DC power converter control', *IEEE Trans. Ind. Electron.*, 2014, **61**, (11), pp. 5987–5995

[4] Din, E., Schaef, C., Moffat, K., *et al.*: 'A scalable active battery management system with embedded real-time electrochemical impedance spectroscopy', *IEEE Trans. Power Electron.*, 2016, **32**, (7), pp. 5688–5698

[5] Bayya, M., Rao, U.M., Prabhakara, B.V.S.S.N., *et al.*: 'Online battery monitoring using model based approach – impedance'. 2015 Int. Conf. on Industrial Instrumentation and Control (ICIC), Pune, India, 2015, pp. 1630–1634

[6] Qahouq, J.A.A.: 'Online battery impedance spectrum measurement method'. 2016 IEEE Applied Power Electronics Conf. and Exposition (APEC), Long Beach, USA, 2016, pp. 3611–3615

[7] Thanh-Tuan, N., Van-Long, T., Woojin, C.: 'Development of the intelligent charger with battery state-off-health estimation using online impedance spectroscopy'. 2014 IEEE 23rd Int. Symp. on Industrial Electronics (ISIE), Istanbul, Turkey, 2014, pp. 454–458

[8] Depernet, D., Ba, O., Berthon, A.: 'Online impedance spectroscopy of lead acid batteries for storage management of a standalone power plant', *J. Power Sources*, 2012, **219**, pp. 65–74

[9] Zhao, L., Fu, Q., Liu, Z.: 'An electrochemical impedance spectroscopy measurement system for electric vehicle batteries'. 2016 35th Chinese Control Conf. (CCC), Chengdu, China, 2016, pp. 5050–5055

[10] Wang, X., Wei, X., Dai, H., *et al.*: 'State estimation of lithium ion battery based on electrochemical impedance spectroscopy with on-board impedance measurement system'. 2015 IEEE Vehicle Power and Propulsion Conf. (VPPC), Montreal, Canada, 2015, pp. 1–5

[11] Cho, S.-Y., Lee, I.-O., Baek, J.-I., *et al.*: 'Battery impedance analysis considering DC component in sinusoidal ripple-current charging', *IEEE Trans. Ind. Electron.*, 2016, **63**, (3), pp. 1561–1573

[12] Tröltzsch, U., Kanoun, O.: 'Miniaturized impedance measurement system for battery diagnosis'. Proc. SENSOR 2009, Nürnberg, Germany, 2009, Vol. I, pp. 251–256

[13] Varnosfaderani, M.A., Strickland, D.: 'Online impedance spectroscopy estimation of a battery'. 2016 18th European Conf. on Power Electronics and Applications (EPE'16 ECCE Europe), Karlsruhe, Germany, 2016, pp. 1–10

[14] Katayama, N., Kogoshi, S.: 'Real-time electrochemical impedance diagnosis for fuel cells using a DC-DC converter', *IEEE Trans. Energy Convers.*, 2015, **30**, (2), pp. 707–713

[15] Koch, R., Riebel, C., Jossen, A.: 'On-line electrochemical impedance spectroscopy implementation for telecommunication power supplies'. 2015 IEEE Int. Telecommunications Energy Conf. (INTELEC), Osaka, Japan, 2015, pp. 1–6

[16] Din, E., Schaef, C., Moffat, K., *et al.*: 'Online spectroscopic diagnostics implemented in an efficient battery management system'. 2015 IEEE 16th Workshop on Control and Modeling for Power Electronics (COMPEL), Vancouver, Canada, 2015

[17] Ahmed, A.: 'Series resonant switched capacitor converter for electric vehicle lithium-ion battery cell voltage equalization', Masters thesis, Concordia University, Montréal, Québec, Canada, 2012

[18] Varnosfaderani, M.A., Strickland, D.: 'Online impedance spectroscopy estimation of a DC–DC converter connected battery using an earth leakage monitoring circuit'. 19th European Conf. on Power Electronics and Applications (EPE'17 ECCE Europe), Warsaw, Poland, 2017

[19] Yuanmao, Y., Cheng, K.W.E., Yeung, Y.P.B.: 'Zero-current switching switched-capacitor zero-voltage-gap automatic equalization system for series battery string', *IEEE Trans. Power Electron.*, 2012, **27**, (7), pp. 3234–3242